A Design Overview of a Space-Based Chromotomographic Hyperspectral Imaging Experiment

Todd A. Book, William J. Starr, Arthur L. Morse, and Steven D. Miller
Graduate Students, Air Force Institute of Technology
Wright Patterson AFB, OH 45430; (937)-785-3636 ext 4578
todd.book@afit.edu

Jonathan T. Black, Eric D. Swenson, Richard G. Cobb and Carl R. Hartsfield
Assistant Professors, Air Force Institute of Technology
Wright Patterson AFB, OH 45430; (937)-785-3636 ext 4578
jonathan.black@afit.edu

ABSTRACT

Hyperspectral imagery (HSI) has largely been developed to monitor static scenes or slowly changing events. To provide an additional responsive space-based capability, a novel spectrometer that can characterize highly-transient events is proposed. Chromotomography (CT) is a technology that enables HSI to detect and classify fast transient combustion events. An experimental space-based CT imager is currently being constructed at the Air Force Institute of Technology (AFIT). The space-based CT imager is being designed as a small payload that will operate from the Exposed Facility (EF) of the Japanese Experimental Module (JEM) on the International Space Station (ISS). The collected data from the space-based experimental payload will validate the science of CT and demonstrate the multifunctional applications of the instrument.

INTRODUCTION

Hyperspectral imaging is a valuable tool that combines spatial and spectral information from a target of interest, which can be exploited for scientific and military purposes. Traditional hyperspectral imaging, until recently, was only able to image static or slowly changing scenes. It was not able to combine a rapid temporal dimension with the spectral and spatial dimensions. There is current interest in being able to image fast transient combustion events of less than 0.1 sec as shown in Figure 1 using hyperspectral imaging. However, to image fast transient events, an imager must be able to successfully collect spatial, spectral and rapid temporal information at a rate equal to or greater than 10 Hz.

Chromotomography is one type of technology that can be used to image fast transient events in addition to others, such as Fourier Transform Spectroscopy (FTS). Chromotomography enjoys several advantages over FTS including less sensitivity to vibration, simpler integration, and increased temporal response[1]. The scientific concept for chromotomographic hyperspectral imaging originated with the Air Force Research Laboratory (AFRL) and Solid State Scientific Corporation (SSSC)[2].

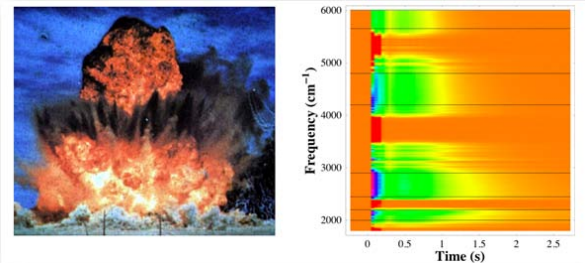

Figure 1: Example of a Transient Combustion Event's Spectral Signature

This paper describes the design and concept of operations of the Space Chromotomography Experiment (CTEx) intended to be flown on the International Space Station's (ISS) Japanese Experimental Module Exposed Facility (JEM-EF).

BACKGROUND

Chromotomography Theory

At the center of AFIT's chromotomographic experiment is a rotating prism and algorithmic transforms similar to medical tomography to reconstruct the data.

Most hyperspectral imagers use gratings to separate incoming wavelengths. Prisms used in chromotomography are a simpler device that can perform the same function to disperse the wavelengths of a collected spatial scene onto the Focal Plane Array (FPA). By rotating the prism, the spectral information is dispersed on the FPA at different angles, thus allowing the scene's spatial and spectral content to be reconstructed using tomography. In theory, in order to sample transient combustion events with a finite life of approximately 0.1 sec, the prism would have to spin at a rate equal to 10 Hz. Each prism rotation angle captured by the imager corresponds to a single spectral wavelength comprising the hyperspectral data cube.

The actual operation and theory of the CTEx instrument is of interest to understand how a chromotomographic hyperspectral imager works. Figure 2 represents how the spectral points for a spatial pixel source lie along a line and why the spacing along the line is important. The collimated Hg point source is dispersed by the prism by wavelength as a line onto the camera array. The spectral signature of the collimated Hg point source and the dispersion by the prism determines where the signature is recorded along the spectral line on the array. The location along the line represents the spectral wavelength of the source. Figure 3 provides an example of the theoretical spectral dispersion of the CTEx prism.

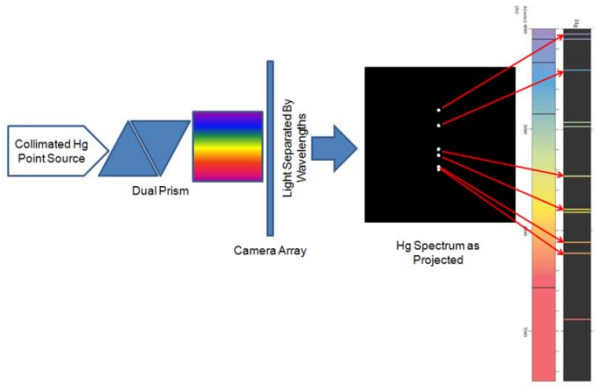

Figure 2: Spectral Dispersal of an Hg Point Source

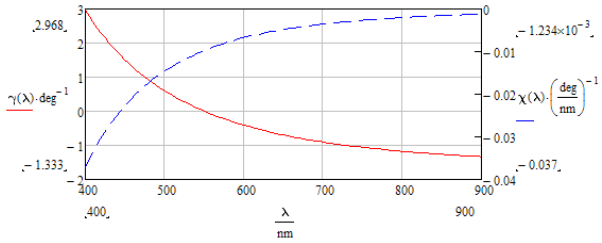

Figure 3: Theoretical Spectral Dispersion of the CTEx Prism[3]

In Figure 4, the image is a composite of over a hundred different images of the Hg point source, each at a different prism rotation angle, overlaid on top of each other. The prism is rotated in order to allow for the chromotomographic data to be reconstructed into a traditional spectral cube. The center of rotation in Figure 4 represents the undeviated wavelength of the spatial pixel being imaged. This is the wavelength path that is not altered by the prism as shown in Figure 3. For the ground-based CTEx the undeviated wavelength is approximately 550 nm.

Figure 4 : Spectral Dispersion of Each Prism Position Overlaid as a Single Image Using Simulated Data

Figure 5 represents the final concept on how the algorithm takes the raw image data and reassembles a traditional spectral cube for each pixel. It shows an example of how two spectral wavelengths are reconstructed for a single spatial pixel using the chromotomographic data. Since each location from the center of rotation represents a wavelength, the reconstruction algorithm uses a frame of the wavelength location at each prism angle. For simplicity,

only eight prism angles are represented in Figure 5. The frames are then dragged to the spatial pixel location, which is the center of rotation, and overlaid on top of each other to form a single spectral image for that wavelength and pixel. Since adjacent spatial pixels would add noise to each frame, the images are overlaid. In the case here, only a single spatial pixel is shown corresponding to the Hg point source, but in reality, the field of view would contain numerous spatial pixels that would add noise to the reconstruction process. To overcome this noise, more prism angles are imaged and more images are overlaid causing only spectral features for that spatial pixel to show up.

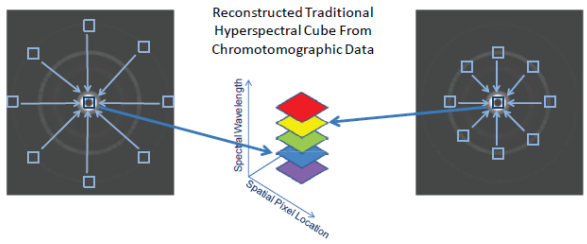

Figure 5 : Re construction o f Si mulated Chromotomographic Data i nto a Traditional Hyperspectral Cube

The full CTEx program is broken into three phases: a lab-based experiment, a ground-based instrument, and the spaceflight experiment.

Lab-Based CTEx

Figure 6 contains a schematic of the lab-based CTEx instrument[4], which consists of a telescope (L1 and L2), rotating direct vision prism (DVP), focusing lens (L3) and a detector array. The goals of the experiment included[1]:

- Construction of a chromotomographic hyperspectral imaging device
- Detailed performance characterization
- Demonstrate the capability to collect, process and exploit the spectral imagery for a primarily static spectral target

Descriptions of the lab experiments can be found in References 1 and 4.

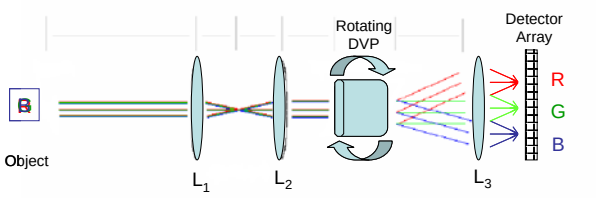

Figure 6: Schematic of L ab-Based C TEx Instrument[1]

Ground-Based CTEx

Figure 7 contains a picture of the completed ground instrument[5]. The main goals of the ground-based experiment included:

- Construction of a ground-based chromotomographic hyperspectral imaging device
- Demonstrate proof-of-concept outside the lab in a field environment using a changing spectral target at some distance

Details of the instrument and collected data can be found in Reference 5.

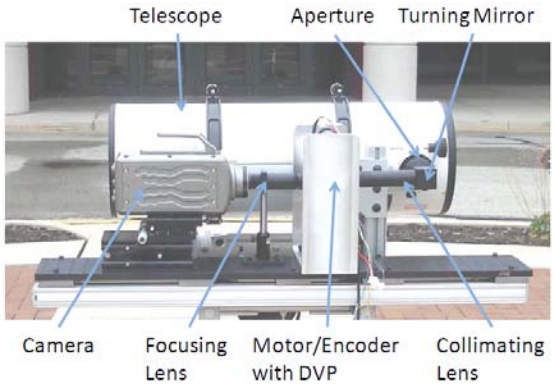

Figure 7: Completed G round-Based CTEx Instrument[5]

Space-Based CTEx

The initial research into the development of the space-based chromotomographic imaging experiment has begun. This article will highlight the current research that has been completed at AFIT for the design and fabrication of this instrument. For the space-based experiment, the system is designed to interface with the Exposed Facility of the Japanese Experiment Module on the International Space Station. On the ISS, the experiment will operate independently of the astronaut crew. The main goals of the space-based experiment include:

- Construction of a spaced-based chromotomographic hyperspectral imaging device that interfaces with the JEM-EF
- Demonstrate a low-cost multi-functional chromotomographic imaging spectrometer that will provide visible-infrared (VIS-IR) hyperspectral imagery for transient combustion event classification

- Raise the technology readiness level of chromotomographic hyperspectral imaging to six

Three characterizations of different scenes are planned to achieve these goals. These objective collects are:

- Static hyperspectral scene, such as a tank through the trees
- Point source transient event, such as a salt emission line characterization of a burner
- Large transient event, such as a forest fire

Exposed Facility (EF) of the Japanese Experiment Module (JEM)

The space-based CTEx is being design for integration with the EF on the JEM shown in Figure 8. This arrangement is beneficial and economical, because it allows the experiment to use ISS power, communications, and orbital maintenance. The EF is designed as a microgravity experimental facility with minimal vibration levels, which are ideal for the space-based CTEx instrument.

Once connected, the EF will provide all the support that the space-based CTEx requires without astronaut interaction, because the payload will receive command and control from AFIT. The primary power supplied to each payload is 3KW at 120V DC with a max load of 25 amps. A separate payload survival power supply provides 120 W at 120V DC with a max load of 1 amp. Each payload has a separate 10 Mbps medium Ethernet channel for data download[6]. The ISS will provide the orbital maintenance for the experimental until it is completed and disconnected from the EF for disposal by allowing it to burn up during reentry. The EF of the JEM is currently used by a another experimental his payload, the Hico-Raids Experimental Payload (HREP)[8].

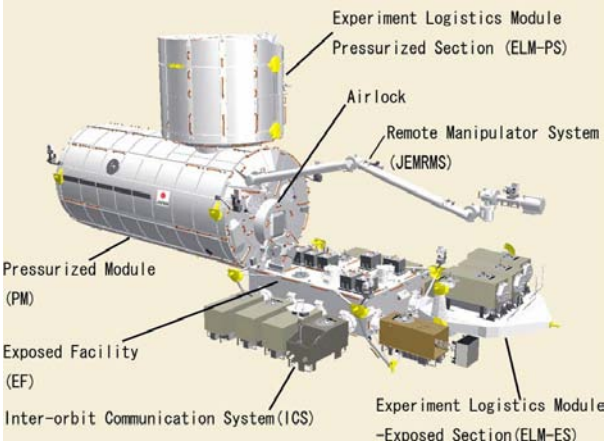

Figure 8: Japanese Experimental Module with Exposed Facility[7]

SLEWING, ATTITUDE DETERMINATION, AND POINTING STUDY

To generate and verify specifications for the space-based CTEx hardware, it was necessary to conduct a slewing, attitude determination and pointing study. This analysis was conducted using actual two line element sets (TLEs) covering a period of six months from 10 April 2009 to 15 October 2009. The invariant altitude (IA) of the station is used throughout this analysis, which is the mean altitude of each orbit. The IA removes the small differences in altitude caused by the slight eccentricity of the orbit and the shape of the Earth. During this time period, the IA of the ISS ranged from 346 km to 352 km. These results were then used to develop the mission plan for CTEx from launch to experimental data collection and downlink, which is discussed later.

In-Track Slewing

During the CTEx telescope design, the decision was made to slew the instrument in-track using a slow steering mirror with a range of ±8 deg. This range meets the required collection time of 10 sec as shown by the associated on-orbit sensor parameters in Table 1, where FOV is the circular field of view of the instrument, R is the radius of the FOV, V_c is the circular velocity, T is the orbit period, V_{gt} is the velocity of the subsatellite point, $t_{nadirview}$ is the time the object will be in view with a fixed telescope, and ω is the required slewing rate. This analysis used an altitude of 350 km and assumes the orbit to be circular. Although the station's orbit is not exactly circular, it was a reasonable assumption since its eccentricity is 0.0009, as reported in the TLEs.

Table 1: On-Orbit Sensor Parameters

	Altitude	
	350 km	**450 km**
FOV_{nadir} [km^2]	0.293	0.484
$2R$ [m]	610.9	785.4
R [m]	305.4	392.7
$FOV_{off\text{-}nadir}$ [km^2]	298.9	484.5
$2R$ [m]	616.9	785.4
R [m]	308.4	392.7
V_c [km/s]	7.697	7.640
T [min]	91.538	93.586
V_{gt} [km/s]	7.297	7.137
$t_{nadirview}$ [s]	0.0837	0.110
ω [deg/s]	1.26	0.973

The in-view time for two target locations, Dayton Ohio and Mt. Washington, was deterimined using the dwell mirror in-track slewing range, ±8 deg. This range enables CTEx to track a target and collect data for approximately 14 seconds at the current altitude of 350 km. At 450 km, CTEx will be able to view a target and collect data for approximately 17 seconds. The next section will focus on the cross-track slewing requirement.

Cross-Track Slewing

The cross-track slewing requirement was analyzed through the production of access reports. Table 2 lists the number of accesses to each target site (no lighting constraints) and each United States Geological Survey (USGS) calibration site (direct sunlight) for each sensor slewing configuration at both the current altitude of 350 km and the planned altitude of 450 km. In several cases, the number of calibration site accesses for a given sensor actually decreases when the altitude of the station is increased. This seems counterintuitive; however, the decrease in site access is due to the lighting constraint. There are actually more accesses, but they occur during periods when the site is not illuminated by direct sunlight.

Table 2: Number of Accesses to Each Site over a Six Month Period

	Number of Accesses					
	0 deg		8 deg		13 deg	
	350 km	450 km	350 km	450 km	350 km	450 km
Dayton, OH	0	0	38	39	59	60
Mt. Wash., NH.	0	0	39	47	62	76
Algeria 3	0	0	18	14	30	30
Algeria 5	0	0	10	12	19	27
Frenchmann Flat	0	0	17	15	28	35
Libya 1	0	0	15	13	27	19
Libya 4	0	0	15	14	22	23
Mauritania 1	0	0	11	13	15	15
Mauritania 2	0	0	8	14	15	23

The fact that there were zero accesses to any of the sites over the six month period without cross-track slewing capability on the instrument indicates that CTEx must slew in the cross-track direction. The slewing range selection is a matter of satisfying mission requirements and system design. CTEx is a proof of concept scientific experiment and does not require a high revisit rate; therefore, either of the slewing options in Table 2 are acceptable.

The ±8 deg slewing capability of the selected dwell mirror allows CTEx to attain the highest level of simplicity by controlling all of the experiment's movement with one set of controllers and motors. This configuration was used for the remainder of this research. Utilizing two controllers, one for each axis, for the dwell mirror maximizes precision. The dwell mirror in the telescope is capable of slewing ±8 deg in each axis and achieves an acceptable number of accesses over both the target and calibration sites. All of the other options require the acquisition and integration of a rotation stage to control the cross-track slewing. This option increases complexity as well as places a potential strain on spatial constraints within the experiment housing.

Attitude Determination

This section covers the results of the attitude determination system analysis. The ISS's planned future altitude of 450 km was used throughout the calculations and modeling.

ISS Position and Attitude Accuracy

The attitude determination accuracy for the ISS is within ±3 deg while the JAXA-KIBO module's – to which the JEM-EF is attached – accuracy is within 0.3 degrees[9]. Table 3 shows the impact that these errors have on the target falling within the sensor's field of regard. The ±3 deg of error in ISS attitude results in nearly a 33 percent reduction in the target falling within the field of regard of the sensor for two of the sites. Reducing this error to ±0.3 deg yields less than a 10 percent reduction. The reduction percentages were calculated by taking the average of the reduced accesses for each attitude accuracy across all sites. Although this seems to be an acceptable level of performance, it is not. These statistics only show that a target will still fall within the field of regard, not the FOV. The following section discusses the accuracy required to ensure that a target actually falls within the FOV of CTEx.

Table 3: Impact of ISS Attitude Knowledge on CTEx Field of Regard

	# of Accesses	Potentially Missed Accesses	
		±3 deg error	±0.3 deg error
Dayton, OH	39	16	3
Mt. Wash., NH.	47	17	0
Algeria 3	14	1	0
Algeria 5	12	5	0
Frenchmann Flat	15	0	0
Libya 1	13	2	0
Libya 4	14	5	1
Mauritania 1	13	2	0
Mauritania 2	14	14	0

Required Attitude Knowledge of CTEx

CTEx has a small FOV radius of 392 m, corresponding to its 30.5 cm dia primary mirror. At an altitude of 450 km and an off-Nadir angle of 8 deg, the diameters of the FOV of the sensor are approximately 785 m and 793 m at Nadir and 8 deg off-Nadir respectively, as shown in Table 1. The small FOV means that small error in the attitude will result in unacceptable pointing accuracy and no target acquisition. Eq. (1) was used to determine the pointing accuracy required to ensure that a target falls anywhere within the sensor's FOV,

$$R = h\tan(\theta) \rightarrow \theta = \arctan(\frac{R}{h}) \quad (1)$$

where R is the FOV radius, h is the altitude, and θ is the angular FOV, which is calculated in Eq. (2).

$$\theta = \arctan(\frac{0.392\text{km}}{450\text{km}}) = 0.05\text{deg} = 180\text{arcseconds} \quad (2)$$

This value of θ could result in the target being on the far edge of the FOV. However, the acceptable level of pointing accuracy required is assumed to be half the radius of the FOV. Using Eq. (2) but instead using R = 196m, we solve for the acceptable pointing accuracy in Eq. (3).

$$\theta = \arctan(\frac{0.196\text{km}}{450\text{km}}) = 0.025\text{deg} = 90\text{arcseconds} \quad (3)$$

Increasing the precision of the pointing accuracy from 180 arcseconds to 90 arcseconds ensures that a target will lie within the central region of the FOV. This helps to limit the chance that system jitter will prevent target acquisition and data collection over the 10 second collection time. A star sensor will be incorporated into the instrument to provide much greater attitude determination accuracy than can be provided by the ISS.

TELESCOPE DESIGN

The telescope selected for the experimental space-based CT instrument is an off-axis Mersenne. This design was selected for several reasons. The off-axis Mersenne telescope design is compact to fit within the dimensional requirements of an EF payload, allows appropriate room for the incorporation of a field stop at the focus point, and allows the light to be collimated at the telescope output prior to the rotating prism[10].

Figures 9 and 10 provide an overview of the off-axis Mersenne telescope design. The telescope is constructed on a zero coefficient of thermal expansion (CTE) breadboard. A zero CTE breadboard was selected after thermal analysis showed that an aluminum breadboard would introduce optical aberrations when subjected to thermal cycling of -30 to +80 ^{o}C. The outer enclosure and internal baffling are fabricated from aluminum. Two off-axis parabolid (OAP) mirrors are the primary optical components for the system.

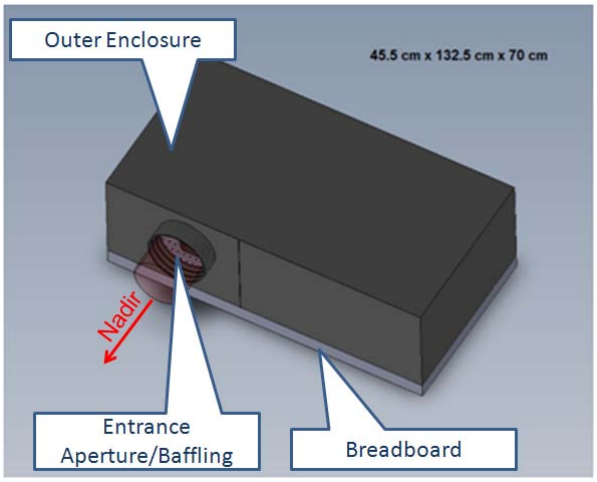

Figure 9 : CAD Dr awing of O ff-Axis M ersenne Telescope Enclosure[11]

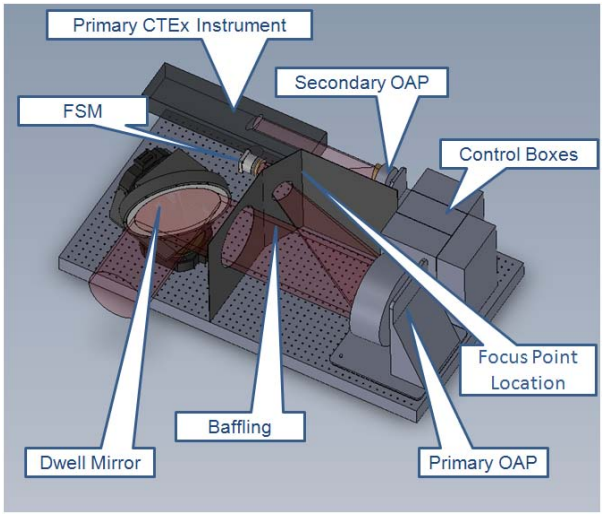

Figure 10: CAD Drawing of Off-Axis Mersenne Telescope[11]

The baffling and enclosure shown in Figures 9 and 10 are intended to prevent any stray light from entering the telescope. The overall enclosure is designed to keep stray light out of the imager, but it is still possible for off-axis light to enter the imager through the entrance aperture. Two bafflings are used to prevent off-axis stray light. The first is located protruding from the entrance aperture of the enclosure. The second baffling is internal and only lets on-axis light pass between the dwell mirror and the FSM. Together both the enclosure and internal baffling should eliminate any stray light from entering the primary CTEx instrument.

Several mechanisms are incorporated into the instrument design. The first is a two-axis dwell mirror, which is capable of providing ±8 deg of steering IAW the previous slewing study. Rather than using a traditional azimuth/elevation mechanism, it is constructed using two rotary stages connected with a wedge to provide a lower profile as shown in Figure 11. The fast steering mirror (FSM) is a tip/tilt platform to correct for jitter due to ISS vibrations. At the focus point location, a precision micro-translation stage was incorporated as a linear actuator for the field stop slide bar. The field stop slide bar contains three different size apertures and a secondary focus target. Four controllers are shown in Figure 10; two for the dwell mirror, one for the FSM and one for the micro-translation stage. All mechanism selected are vacuum qualified, but have to space qualified with the final telescope assembly to date.

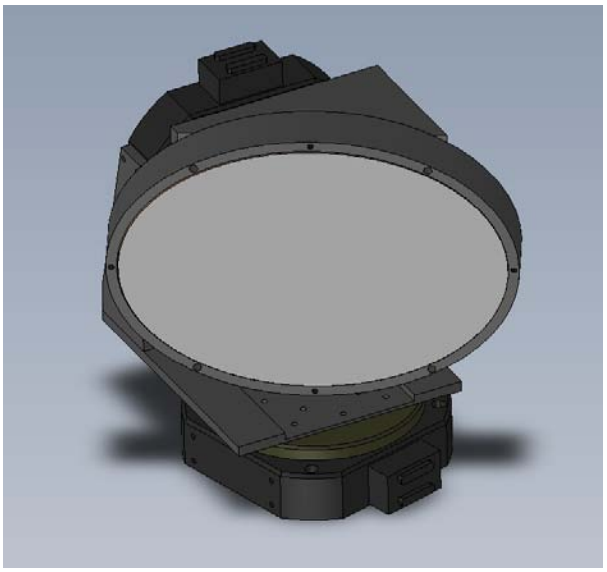

Figure 1 1: CAD Dr awing o f Dw ell Mirror Assembly[11]

Of primary interest are the telescope's optical properties in Table 4 and its associated performance. The two OAP mirrors are the primary optical elements for the telescope. The 23 cm primary OAP and 7 cm secondary OAP yield a 4.65 times magnification and 0.191 degree angular field of view for the telescope. The root mean squared (RMS) wavefront error (WFE) is within the two times diffraction limit for the entire FOV with the exception of 400 nm at the FOV limits which just barely exceeds this requirement. The diffraction exception at the FOV limits for 400 nm is also shown by analyzing the Optical Path Differences (OPD) showing that the increase in WFE at the outer FOV is a gradual rather than an abrupt change. However, given that the maximum angular FOV that will be utilized by CTEx is constrained to 0.05 degrees, the results are acceptable and within diffraction limits. The Modulation Transfer Function (MTF) analysis shows no sharp drop offs as angular frequency is increased for the on-axis FOV and the off-axis FOVs,

which is expected for optimal performance. The Point Spread Function (PSF) analysis shows a large amplitude and very narrow width that is expected for optimal performance. The space-based instrument including the telescope and primary CTEx instrument is designed with a 10 m ground sampling distance (GSD).

Table 4: Optical Properties of the Off-Axis Mersenne Telescope

Property	Value
Entrance Aperture Diameter	20.32 cm
Output Aperture Diameter	5.08 cm collimated
Primary OAP Focal Length	800 mm
Secondary OAP Focal Length	172 mm
Unconstrained Angular FOV	0.191 deg
Constrained Angular FOV	0.05 deg
Magnification	4.65 times
Focus	Fixed, 50 km to ∞
Max RMS Wavefront Error (2 times Diffraction Limit)	0.14

Alignment analysis revealed that the telescope would maintain its optical performance when subjected to minor perturbations in the component alignment from the launch and/or operating environments. Monte Carlo simulations were performed by using 1000 trails with a test wavelength of 632.8 nm to display alignment confidence levels. This analysis showed that with greater than 90 percent confidence, the telescope will maintain its alignment when subjected to perturbations caused by the harsh launch and space environments. The most sensitive optical component in the system shown by this analysis was the alignment of the secondary OAP mirror.

To ensure alignment, a bonding agent was used during fabrication. After the telescope was aligned with an interferometer, the adjustment screws were bonded with epoxy to prevent any future changes in alignment. This epoxy was selected because it is designed for mounting optically sensitive components and has very low outgassing properties.

The telescope fabrication and assembly are only part of the picture. Its integration into the payload structure and space-qualification are critical steps yet to come. Part of its integration into the structure includes a vibration isolation system in conjunction with the FSM to prevent optical jitter.

PASSIVE VIBRATION I SOLATION S YSTEM DESIGN

In optics applications, the design process begins with an optics platform that is extremely stiff. In other words, the platform on which the optics are physically mounted is fabricated to act as much as possible like a rigid body but with very high natural frequencies. A rigid body is ideal for optics as it implies that no point moves with respect to any other point keeping the optical elements in alignment. This optical platform is then attached to the surrounding support structure with an appropriate isolation system which minimizes vibrations from the surrounding structure leaving a stable and relatively low vibration environment for the optics.

A hexapod-like assembly could be designed with six linear isolators, as shown in Figure 12 and made to attach at each point on the optical platform. Simply modifying existing hexapod designs would result in a complex and potentially very large attachment structure as the hardware size required to support six individual attachments would make this concept impractical for the CTEx application. The goal here is to create a less complex isolator that is compact enough to place at each desired attachment point on the platform but allow for isolation and suppression of motion in more than one direction

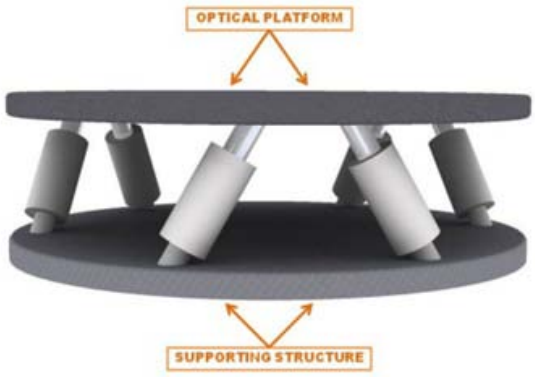

Figure 12: Hexapod V ibration I solation Arrangement[12]

The motivating idea behind this particular design is to take geometrically simple springs and arrange them in such a way as to provide relatively similar characteristics in stiffness and later damping to translation in any three dimensional direction. The geometry also allows for small rotations, though this being a much stiffer motion. The most difficult element of this design is to create the common point to which the three springs and the optical platform would attach. Several concepts involving both rigid elements and rotational joints were examined.

The unique geometric arrangement of the isolator design meant that 3D CAD visualization and prototyping software was the answer to beginning the modeling and analysis of various arrangements and iterations on the design. This process began by designing a base plate and pillar assembly that was easily fabricated and then modifying the initial spring shape to the simplest form.

A thin spring with a constant cross section and with only one bend and two attachment points was created. This left only the design of the central attachment point. After much discussion and exploration of the trade space involving both a rigid and rotational joint as well as their resulting effects on the isolation and suppression of the optical platform of the CTEx instrument, it was decided that a simple rigid center piece would properly complete the design. Using the 3D CAD software, a relatively complex shape was constructed to accept threaded attachments for each of the springs and a larger, single attachment point for the optical platform. The final imager assembly is shown in Figure 13. Due to its appearance, this central attachment device was nicknamed the `jewel' and will subsequently be referred to as such.

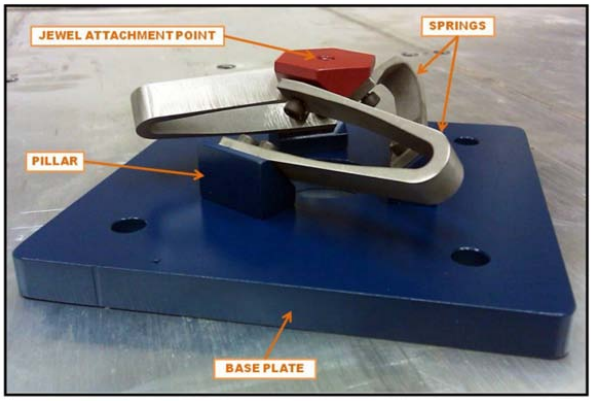

Figure 13: Photograph of the isolator prototype[12]

To test the isolator assembly for use with the CTEx optical platform along with the front end optics, a mock optics platform was produced. The mock platform or breadboard had to be very stiff to mimic the CTEx breadboard. The breadboard had to also represent the nominal weight of the optics platform with appropriate components. In order to accomplish this quickly and with little manufacturing expense, a breadboard design was completed with 0.25 inch thick 6061-T6 aluminum plates placed on either side of an internal frame. The internal frame was created from one inch square t-slot extruded aluminum stock and assembly hardware. With the aluminum plates bolted in place through the internal frame, a stiff platform was created with similar dimensions to the actual CTEx flight hardware and weighing in at approximately 97 lbs.

With the large I-beam attachment on top of the shaker head, as shown in Figure 14 the entire breadboard and isolator assembly was vibe-tested. This setup, with an additional 50 pound mass as shown, was used to test the response of the breadboard as well as the transmittance of the isolators in the vertical direction. The inset in the upper right corner of Figure 14 shows a close-up of the isolator attachment method from the I-beam to the optical platform. Reconfigured and attached to an oil slip table, this shaker was also used to excite the assembly in both the lateral and longitudinal directions.

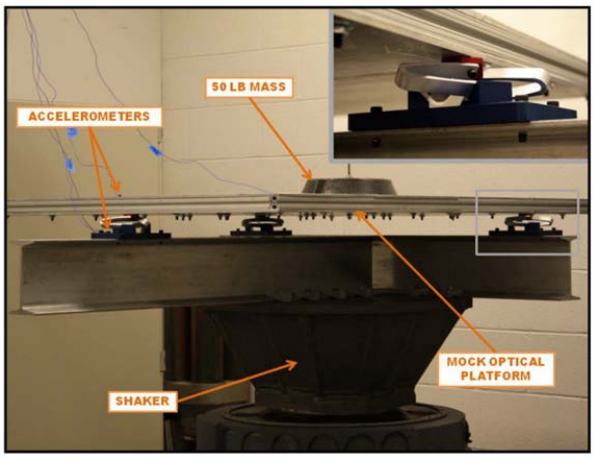

Figure 14: Mock optics platform and isolator assembly on vibration exciter[12]

The triple isolator meets the goal of allowing motion in any direction or rotation and is very compact compared to larger hexapod type designs. The results of the experimental vibration analysis match the predicted behavior of the FE model. The FE model was tuned for the stainless steel springs for both static loads and dynamic analysis. The model was not tuned for either case with the aluminum springs nor was a FE analysis completed for the entire assembly of isolators and mock optical platform. This is a good starting point for better understanding the behavior of the isolators while attached to a larger system where they are designed to work. This analysis should be performed prior to any different approach to passive damping or in consideration for an additional active control system if desired.

The isolator geometry is such that it can easily be varied to eliminate the stiffness directionality of the assembly. Currently, the lateral and vertical translations do not exactly match in terms of natural frequency. However, varying the angle at which the springs are attached to the pillars and jewel (currently 45°) will bring these closer together. Similarly, translational and rotational motion of the jewel is coupled with spring cross-section. Adjusting the width to thickness ratio of the spring cross-section may be used to either bring the

rotational mode frequencies closer to those of the translational modes or further separate them. Together, these properties allow this isolator to be customized to any particular application.

Research and study of methods for providing greater damping to this design is by far the most important area for improvement. The simple rubber dampers experimented with at this point are not ideal and contribute little to the overall design goal. The results of the numerous experiments do indeed conclude that this damping technique is not practical for higher levels of acceleration, though it was important to eliminate this option as it is by far the simplest approach to passive damping with this geometry. The results of the research into this passive vibration mechanism are detailed in Reference 12.

COMPUTER / DATA HANDLING S YSTEM DESIGN

The preliminary electrical design for the space-based CTEx takes some design cues from a couple of current hyperspectral imaging experimental payloads, HREP[13] and ARTEMIS[14]. Additionally, in an effort to keep costs relatively low, commercial off the shelf (COTS) components were used as much as possible in the design of the computer system. The use of COTS parts and not custom designed parts allows for easy procurement of equipment; however, we are limited to what is readily available that is typically older technology. Also COTS equipment is typically not space-rated and further study is needed on the CTEx computer design to evaluate the space environment and possible mitigation techniques.

The first electrical design evaluated was the payload processor on the ARTEMIS spacecraft. After examining this system, it was decided that the use of the compact PCI (cPCI) form factor would be used for CTEx. This is a standard form factor that is used for industrial computers and is convenient because of the readily available ruggedized components. The other design evaluated is the control computer developed for HREP. This design is most closely-related to the system needed on CTEx because HREP is a hyperspectral imager on the EF of the JEM. Because of HREP's location, the communication between the experiment and the ISS is heavily leveraged. Also, the HREP computer uses almost entirely COTS equipment and many components used are not space rated.

For the preliminary design of the central computer of the CTEx system, the Data Collection and Command Unit (DCCU), a compact PCI (cPCI) chassis was chosen. This chassis has a hardened power source and the ability to hold 8 cPCI cards. The processor of the DCCU was chosen for its high interface count and the use of a newer more powerful dual core processor. To complete the interfaces to the rest of the CTEx experiment separate 1553 and digital I/O Industry Pack (IP) cards were chosen. These cards are placed on a cPCI IP carrier card and were chosen because of their small size, two cards can fit onto one carrier. This frees up valuable cPCI slots for future expansion as final designs are fleshed out. The last component of the DCCU is a rugged 128GB Solid State Disk. All of these components go through some level of vibration testing and have an extended operating temperature range, but they are not space qualified. As mentioned above, future work will be needed to evaluate the validity and mitigation techniques of this design choice.

With its multitude of interface types, the DCCU is connected to all of the subsystems of CTEx. The most notable subsystem is the imaging subsystem that is potentially the most taxing subsystem for the computer.

The imaging system of CTEx offers its own unique challenges because of the amount of data being produced by camera. This high speed camera is capable of a maximum of 1.4 million frames per second at a resolution of 128x8 pixels to 8,360 frames per second at 1280x720. The camera has 32 GB of internal volatile memory onboard that CTEx will utilize in order to realize the camera speed needed to adequately develop the HSI data cube. Even with the amount of data coming from the camera, trying to correlate each high-speed image with the angle of the prism at that point in time is very challenging.

In chromotomography, precise knowledge of the angle of the prism during each image is critical to reconstruction of accurate data cubes. To try and help alleviate this issue, a Signal Acquisition Module (SAM-3) was chosen to acquire the data from the spinning prism. The SAM-3 is uniquely helpful in this case because it has the ability to sample digital and analog signals and place them in the header file of each image. This single piece of equipment demonstrates a capability that allows the camera to image the scene and have the precise prism angle recorded as a part of each image. This greatly simplifies the acquisition process and allows the software of the system to be much simpler in scope.

The control software of CTEx is envisioned to be highly flexible, allowing multiple different control schemes for the electronics. The main function of the code shown in Figure 16 has a built in processes to flash the memory in the case of corruption, to calibrate the instrument when needed, and to downlink data at the allotted time. The other aspects of the instrument are handled with calls to four other sub-processes that handle functional testing and data acquisition.

The functional verification test shown in Figure 17 is the first sub-function that the main function calls right after power on and computer initialization. During this process, all of the actuators are centered and initialized, and the camera is fully calibrated. Additionally, all of the current and voltage levels are logged during this test for troubleshooting purposes if needed. The next set of sub-functions that the main function calls are the data acquisition functions. The data acquisition functions are split into three processes: slewing control, camera control, and prism control.

The slewing control function shown in Figure 18 is the most complicated and allows for static, manual, and targeted angles of the dwell mirror. A common thread in each of these modes of operation is a start and stop trigger that is sent to the prism control process. This trigger ensures that the prism is rotating when needed and greatly simplifies the prism control function. For the simplest case, static angle, the user uploads a start and end experiment time and the desired static angle. The system then evaluates the start experiment time and moves the dwell mirror to the specified angle when desired. For manual control, the user uploads a data file that contains times and desired angles. Just as before the system evaluates the time for the first angle and moves the dwell mirror when desired. It then checks for the next angle time or for the end experiment time. The last mode of operation is the targeted mode. In this mode, the user uploads the targets latitude and longitude and the system develops a 3-D acquisition window. This acquisition window is at the altitude of the ISS and is centered on the target with the limits calculated from the slewing limits of the dwell mirror. Once the acquisition window is calculated, the system begins to evaluate the experiment position versus the window. Once inside the window the system slews the dwell mirror to the appropriate angle and begins to continuously update the commanded angle based on position of the experiment and target.

The second process is the camera control function in Figure 19. The camera control function has two modes of operation, time and target. No matter which mode the camera is operating in the user uploads the resolution and speed of the camera. This allows the user to set the camera at any desired setting and allows full use of the camera. For the time mode of operation the function simply uses the start and stop time of the experiment to begin and end image collection. For the targeted mode the function goes through a similar process to the slewing control and develops its own 3-D collection window that has tighter constraints than the acquisition window. The tighter constraints are necessary because of the limited memory space aboard the camera and the desire to not waste valuable space on extraneous images. This collection window is evaluated just like the acquisition window and the camera is turned on and off based on the position of the experiment.

The last process is the prism control function in Figure 20. There are two modes of operation for the process, velocity and manual operation. This function is greatly simplified because of the triggers sent from the slewing control function. For velocity mode the user simply uploads the rotation rate desired for the prism and when the function receives the start trigger, the prism begins to spin until it receives a stop trigger. In manual mode the system looks into a data file uploaded by the user and waits for the trigger to set the first angle. Once the first angle is set the system begins to evaluate the system time versus the time for the next angle. The system then continues down the data file until the stop trigger is received.

ON-ORBIT F OCUS AND CA LIBRATION SCHEME

Focus

There are currently two focus points in the CTEx optical design: one at the field stop location as shown in Figure 10 labeled Focus Point Location and another one at the focal plane array in the primary CTEx instrument. The telescope is being designed with a fixed focus for the first focal point. Since the telescope is fixed focus, changes in the ISS altitude do not need to be accounted for. Analysis of the RMS wave front error (WFE) for the telescope showed that altitudes and slant ranges greater than 50 km will be in focus, because the WFE is less than 2 times the diffraction limit. The active focus control for CTEx is designed to occur at the second focal point on the camera array to correct for any uncertainty.

After launch, the ideal primary method for optimizing focus is by using a vicarious target. ARTEMIS did this using a high spatial frequency scene, like an urban area[15], however, unlike ARTEMIS, CTEx would require the collected images to be processed and reconstructed into traditional hyperspectral cubes before this method could be used. The ideal vicarious focus scheme for CTEx would not require processing first. This can be done with CTEx, by instead of viewing a high spatial frequency scene, using a single sodium street light in a remote location at night. Knowing the theoretical focus setting from the design and ground characterization, a range of focus steps forward and aft of this setting should be selected. A single pass will be done over a remote area with a sodium street light at night while stepping through the range of focus settings. Once this data is down-linked, the scene with the sharpest sodium spectral features

would represent the best focus setting. During the next uplink, the focus setting can be commanded to this position. For redundancy, a focus target is included on the field stop.

A couple of considerations need to be taken into account for focusing the instrument. A lesson from ARTEMIS is that vicarious focus should not be used until after the gains of the individual pixels in the array are averaged with the first vicarious radiometric calibration target because of possible errors without first leveling the pixel gains[15]. Another consideration is that changes in the focus setting have impacts on the calibration because it changes the spectral spread and offset. Impacts to the calibration are easily adjusted for on orbit during the focusing procedure by characterizing the changes in spectral spread and offset on the ground and applying these changes as a rough estimate to the down-linked focusing data cubes.

Calibration

Just like any other scientific instrument, CTEx requires calibration to validate and ensure the integrity of its data. For traditional spectrometers, just spectral and radiometric responses need to be calibrated, however for a chromotomographic hyperspectral imager four characteristics must be measured; offset, spectral spread, undeviated wavelength, and pixel gain. For CTEx, pixel gain (radiometric) calibration is the same as with traditional hyperspectral imagers.

For spectral calibration, several measurements are needed: offset, undeviated wavelength and spectral spread. Figure 15 displays a graphic representation of these three measurements using the spectral lines of a single spatial pixel of a mercury lamp source with prism rotation angles of 0, 90, 180 and 270 degrees. The offset is the measurement in pixels from the center of rotation to the undeviated wavelength, which is the point on the spectral line perpendicular to the center of rotation. The offset can be measured at only one prism rotation angle, but, as shown, this offset may be different for different prism angles creating an ellipse instead of a perfect circle. To currently characterize the offset, four prism rotation angles at 0, 90, 180, and 270 deg are utilized. In order to determine the undeviated wavelength, the spectral spread must first be determined. The spectral spread is calculated by counting the number of pixels between the reference spectral points. In Figure 15, the reference spectral points of a mercury source are 405, 436, 546 and 579 nm. The spectral spread is a nonlinear relationship that allows a spectral wavelength value for each pixel along the spectral line to be determined. Once the offset and spectral spread are determined, the pixel position of the undeviated wavelength can be correlated to a spectral wavelength. Characterization of the offset, spectral spread and undeviated wavelength completes the spectral calibration of CTEx, leaving just the radiometric calibration.

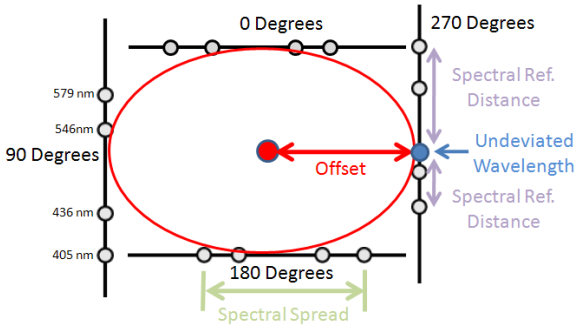

Figure 15: Graphic Depiction of a Mercury Line Source with Prism Rotation Angles of 0, 90, 180, 270 Degrees

For CTEx, it was determined that the best calibration approach was to use both on-board and external calibration approaches. Using this approach seems logical for a traditional hyperspectral imager using the on-board source to monitor calibration trending and the external source for the absolute calibration, but chromotomography has different requirements for calibration.

For chromotomography, the use of an on-board source is initially necessary to characterize the offset, undeviated wavelength and spectral spread after launch. Unmonitored slight changes in these values during launch can have drastic consequences on the ability of the algorithm to deconvolve the collected images. Providing the imager with a known on-board source will make it easier for the ground team to make slight modifications to algorithm's variables by knowing what the deconvolved image should look like to measure the offset, undeviated wavelength and spectral spread. Once the algorithm is updated to take into account any launch changes, vicarious external calibration sources can be utilized to fine tune the spectral and radiometric response of the CTEx imager.

For calibration of the space-based CTEx, three on-board systems will be used. A laser diode calibration system mounted on the aperture cover will be used for initial on-orbit spectral calibration and as required to troubleshoot any technical problems. The four laser diodes provide collimated, narrow spectral sources at 405, 445, 670, and 852 nm. A filter wheel with several narrow bandwidth filters in the optical path will trend the imager's calibration between vicarious calibrations, as well as be inserted to reduce noise in spectrally uniform scenes. The final on-board source will be

several green LEDs (close to the undeviated prism wavelength) placed on the aperture cover to uniformly illuminate the camera array for pixel characterization. Pixel characterization can be performed by capturing a series of images at varying exposure times to the LED source then plotting the pixel responses as a function of the log of the exposure time. This characterization will provide the individual pixel blackout response, gain and non-linear saturation points, as well as identify cold and hot pixels. From this, individual pixel gains across the array can be leveled.

Vicarious (external) calibration will be the primary calibration method for the space-based instrument on-orbit, since spectral and radiometric properties of vicarious targets do not change over time. The space-based CTEx will utilize Earth-based calibration references, since it is unable to slew to view the sun or moon. For spectral features, the space-based CTEx will utilize the atmospheric oxygen A and B absorption features at 762 nm and 687 nm. Both these features are in the spectral range of the CTEx and do not change, unlike H_2O absorption features. For radiometric calibration, the instrument will utilize one of the six United States Geological Survey pseudo-invariant sites to ensure the individual pixel gains are leveled and then the Frenchmann Flat for an accurate radiometric calibration reference[16]. Any of the six pseudo-invariant sites will provide a uniform target that fills the FOV to ensure uniformity of the individual pixel gains. The Frenchmann Flat site was selected as the primary radiometric calibration target because it is instrumented for continuous monitoring. The data for this site is available immediately online and then can be modeled to get the top of the atmosphere radiances to compare to the space-based collection.

MISSION PLAN

This section covers an initial hypothetical mission plan for CTEx. The plan begins with launch on 23 November 2012 and proceeds through data collection and downlinking. The launch date is a date selected at random to serve as a worst case starting point for this analysis. November is a worst case option because the seasons of the year do not align nicely with the desired order of the experiments. Due to the sub-optimal timing, the three experiments will require nearly nine months to complete. This section also assumes that CTEx, like HREP, will fly on the H-II Transfer Vehicle (HTV).

From Launch to Installation on the JEM-EF

It is reasonable to assume that CTEx will closely follow the same timeline that HREP followed. It will take eight days for CTEx to launch and reach the ISS. An additional three days is required to transfer equipment and supplies from the HTV to the ISS. Finally, on days 12 through 14, CTEx will be transferred from the HTV Exposed Pallet (EP) to the appropriate location on the EF.

Installation Complete to Calibration Complete

Following installation of CTEx onto its specified port on the JEM-EF, initialization procedures must be run. Once CTEx is attached to the JEM-EF, the survival power will be turned on followed by the operational power. While powering on, the boot procedures and thermal configuration of the system is monitored. After successfully booting the system, the instrument will be taken out of launch configuration and placed into an operational configuration. Specifically, the mirrors and other mechanical components that are stabilized for launch must be released to enable a full range of motion. Next, the system will be allowed to outgas for seven days. The seven day window was chosen as an initial estimation based on other similar sensors. However, once the final design is complete and a list of materials is available, the outgassing time will need to be calculated. While CTEx is outgassing, stray light within the system can be characterized and noise trending can be accomplished while all of the doors are still closed and the instrument is running. On days 21 through 27, CTEx will conduct initial calibration. These results will be downlinked and analyzed at AFIT to ensure proper focus and calibration. Once these procedures are successfully completed, CTEx is prepared to conduct additional functional testing and routine operations.

Mission Capable through Data Downlink

Once CTEx has successfully completed initial calibration, the data has been analyzed, and final settings have been uplinked to CTEx, the experiment will be considered mission capable. In this phase of operation CTEx will collect event data on a target of opportunity. A target of opportunity is defined as any target that requires no precise cross track slewing. The purpose of this collection is to test the in track motion compensation and evaluate the quality of data with all initial calibration corrections implemented. One possible means of collection is to conduct an absolute calibration because these sites are large and uniform. Next, CTEx will conduct a data collection and downlink of a target requiring cross track slewing. This target should contain readily identifiable features to aid in geolocation of the image. This data will be analyzed on the ground to determine if the intended target was imaged, thus ensuring that the pointing system is

working correctly. Finally, experimental data collections of the planned targets will be conducted, downlinked and analyzed.

Orbital simulations provide some useful information on the revisit time for the sites used for absolute calibration. The median revisit time for Frenchman Flat is 11 days while the minimum and maximum revisit times are four and 23 days respectively. The median revisit time for any one of the six pseudo-invariant sites is two days while the minimum and maximum revisit times are one and 10 days respectively. The median time between any one of the six pseudo-invariant sites and the next access of Frenchman Flat is six days while the minimum and maximum times are one and 16 days respectively. These revisit times drive the planning window for calibration of the sensor to consume seven days.

Conduct of Planned Experiments

After the first 91 days in operation, CTEx will be fully initialized and calibrated and ready to collect experimental data. The objective collects are the static hyperspectral scene, the large transient event, and the point source transient event. The target site locations of Dayton, OH and Mt Washington, NH are comprised of primarily deciduous trees at low altitude. The absence of leaves in the months of February and March make these optimal times for the point source transient event collection. The large transient event is templated to be a forest fire or other large combustion event. The height of the forest fire season runs from mid to late summer, making this the optimal time for the large transient event collect. Therefore the order of experiments is the point source transient event, the static hyperspectral scene, and the large transient event.

The point source transient event collection can be established at either target location. Each site experiences an average of 25 days of clear or partly cloudy days during the month of March[17]. Using the orbital simulation, it was determined that the Dayton, OH and Mt Washington, NH will be visible for five days and seven days respectively during the month of March.

The static hyperspectral scene can be accomplished at either Dayton, OH or Mt Washington, NH. In this simulation, the experiment takes place at Dayton, OH and has a primary and secondary collection opportunity planned for 12 Apr. This experiment consists of imaging a specific location in an effort to discriminate a camouflaged vehicle from surrounding vegetation.

There is a break in the timeline between the static hyperspectral experiment and the large transient experiment. This break is due to the time of the year and the low probability that there will be a forest fire prior to the summer months. This time period can be used to repeat other experiments or to execute collections on targets of opportunity.

The site of the large transient event was arbitrarily chosen to be a historic site of the fires located to the Northeast of Los Angeles, CA in the Angeles National Forest. During the months of July and August, the Angeles National Forest is accessible to CTEx a total of eight times. The combination of the intermittent clouds and the smoke from the fire may hinder collection slightly, but the long window for collection increases success.

Mission Plan Summary

As mentioned earlier, this is a worst case scenario analysis with a November launch date. It will take approximately 15 days from launch until CTEx is installed on the JEM-EF; the initialization of the instrument will take approximately 35 days; the initial data collection and characterization of the system will take approximately 40 days. Assuming results are favorable at the conclusion of the first 91 days, CTEx will be capable of providing reliable chromotomographic hyperspectral data for other experiments. The three experiments will require approximately 170 days to complete given a launch date in November. This timeline is primarily driven by the conditions required to execute each of the three experiments. The large transient event, a forest fire, requires that it be fire season. The primary plan for a large fire should be to plan a controlled burn. Controlled burns occur on a regular basis on Army installations and throughout the forestry service. The back-up plan should be to image naturally occurring fires. These natural fires may provide several data collection opportunities in addition to any planned controlled burns. The point source transient event can be conducted at any time of the year. The static hyperspectral scene requires that there be sufficient naturally occurring vegetation to render a man-made object indistinguishable from the surroundings to the naked eye. Although this timeline is significant, it is not unreasonable to request an on-orbit life of one year for a JEM-EF payload.

Perhaps the most important planning factor in accomplishing the three experiments within the NASA planning scheme is the programming of multiple target collection opportunities for each experiment. Programming for and collecting against multiple targets for a single experiment will increase the probability of a successful experiment given possible pointing errors

and cloud cover over the targets. Of course this requires sufficient data storage capabilities and increases the desire to have some form of on-board processing that can, at least, determine if the target was detected during the collection opportunity.

CONCLUSIONS

The space-based CTEx instrument is being assembled at AFIT. The sub-components are currently undergoing design and/or fabrication. The delivery of the telescope assembly recently marks a milestone as the arrival of the first complete major sub-assembly.

The usefulness of CT technology has already been proven in the lab and on the ground, resulting in the space-based CTEx being ranked by the 2009 DOD Space Experiments Review Board for launch priority. It is expected as the instrument nears the end of its design and fabrication that it will receive a launch date. This experiment will use a novel COTS design to perform the first hyperspectral characterization of rapidly-transient combustion events from space. The successful completion will prove the CT technology and science and serve as a risk reduction for future operational systems.

REFERENCES

1. Bostick, R. L. and Perram, G. P., “Hyperspectral Imaging Using Chromotomography: A Fieldable Visible Instrument for Transient Events," International Journal of High Speed Electronics and Systems, Vol. 18, No. 3, 2008.
2. Murguia, J. E., Reeves, T. D., Mooney, J. M., Ewing, W. S., Shepherd, F. D. and Brodzik, A. K., “Compact visible/near-infrared hyperspectral imager," Infrared Detectors and Focal Plane Arrays VI , edited by E. L. Dereniak and R. E. Sampson, Vol. 4028, SPIE, 2000, pp. 457-468.
3. Hawks, M. R., “CTEx Optical Design Notes," 2009, Unpublished work of LtCol Michael Hawks, Engineering Physics Department, Air Force Institute of Technology.
4. Bostick, R. L., Perram, G. P., and Tuttle, R., “Characterization of spatial and spectral resolution of a rotating prism chromotomographic hyperspectral imager," Next-Generation Spectroscopic Technologies II , edited by M. A. Druy, C. D. Brown, and R. A. Crocombe, Vol. 7319, SPIE, 2009, p. 731903.
5. O’Dell, Daniel C., Bostick, Randy, Hawks, Michael R., Swenson, Eric D., Black, Jonathan T., and Perram, Glen P., “Chromotomographic Imager Field Demonstration Results,” Airborne Intelligence, Surveillance, Reconnaissance (ISR) Systems and Applications VII Conference, SPIE, 2010.
6. Japanese Aerospace Exploration Agency, “JEM Payload Accommodation Handbook: Exposed Facility/Payload Standard Interface Control Document,” Vol. 3, NASDA-ESPC-2900A, Apr. 2007.
7. NASA, “Japanese Experimental Module,” NASA Homepage, Mar. 2010. http://spaceflight.nasa.gov/gallery/images/station/jem/hires/jsc2003e42552.jpg
8. NASA, “Japanese Experimental Module,” NASA Homepage, Mar. 2010. http://www.nasa.gov/mission_pages/station/science/experiments/HREP-HICO.html
9. Hatton, J., “Call for Ideas Annex 1: Experiments for Global Climate Change from the ISS," Tech. rep., HSF-US/ESA-ESTEC, 2009.
10. Sheirich, P., An Engineering Trade Space Analysis for a Space-Based Hyperspectral Chromotomographic Scanner, Master's thesis, Air Force Institute of Technology, Wright-Patterson AFB, March 2009.
11. RC Optical Systems, AFIT CTS Platform Update, December 2009, Teleconference between AFIT and RC Optical Systems with associated slides.
12. Miller, Steven D., Swenson, Eric D., Cobb, Richard G., Black, Jonathan T., Hartsfield, Carl R., Book, Todd A., Starr, William J., and Morse, Arthur. “Investigation of a Novel Compact Vibration Isolation System for Space Applications.” 51st Structures, Structural Dynamics, and Materials Conference (SDM), AIAA Paper 2010-2935, 2010.
13. Cliford, G., "HICO/RAIDS Experiment Payload (HREP)," Presentation provided to AFIT, Jan 2010.
14. Troxel, I., Fehring, M., and Chenoweth, M., "Achieving Multipurpose Space Imaging with the ARTEMIS Reconfigurable Payload Processor," Proc. Aerospace Conference, 2008.
15. Chrien, T., Schiller, S., Silny, J., and Lockwood, R. B., \On-Orbit Calibration and Focus of Responsive Space Remote Sensing Payloads," 4th Responsive Space Conference, AIAA, Los Angeles, CA, April 2006.
16. United States Geological Survey, USGS Catalogue of Worldwide Test Sites for Sensor Characterization, November 2009, http://calval.cr.usgs.gov/sites-catalog-map.php
17. Dellinger, D., “Cloudiness-Mean Number of Days," Available at http://lwf.ncdc.noaa.gov/oa/climate/online/ccd/cldy.html, 2008.

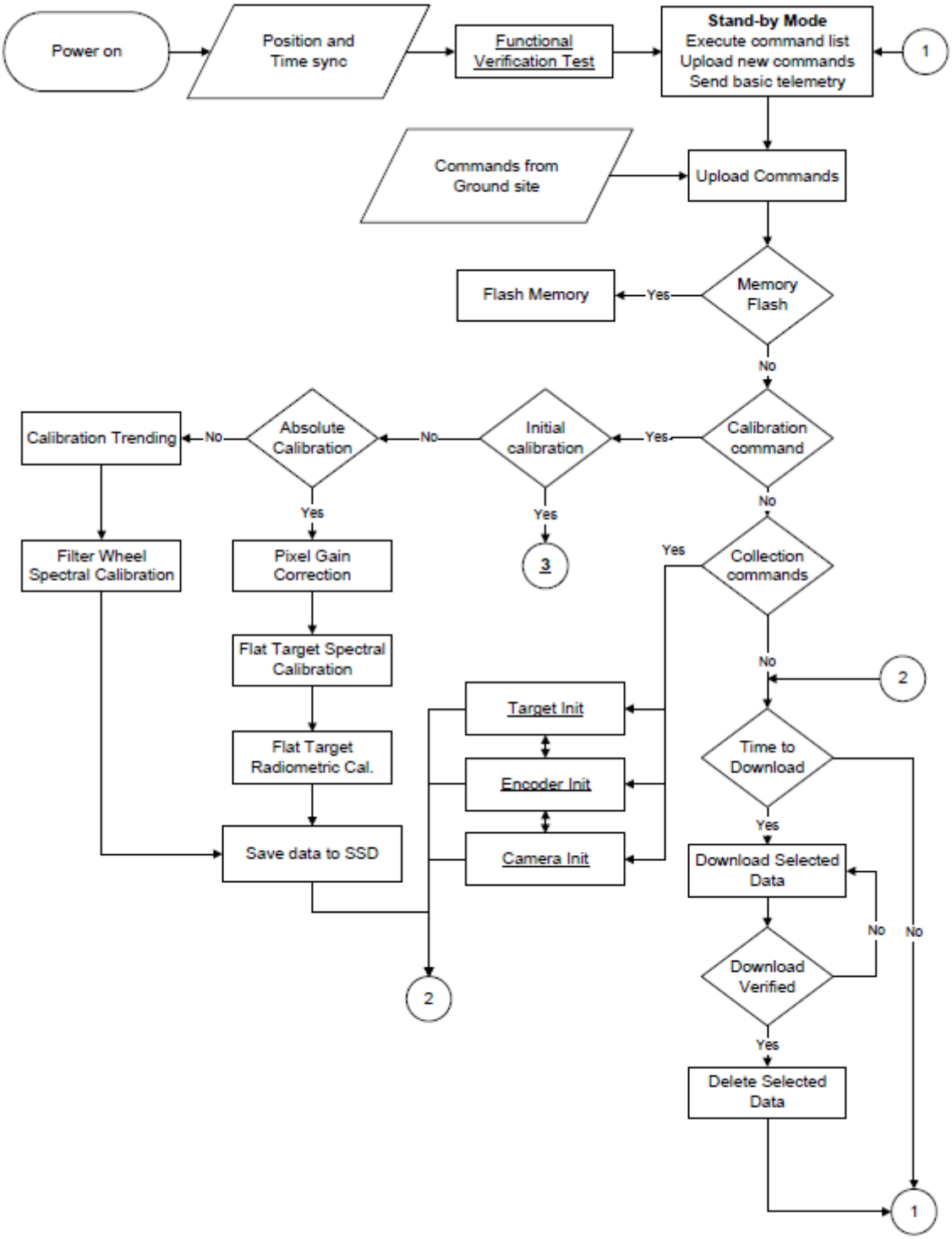

Figure 16: Space-Based CTEx Overall Flow Diagram

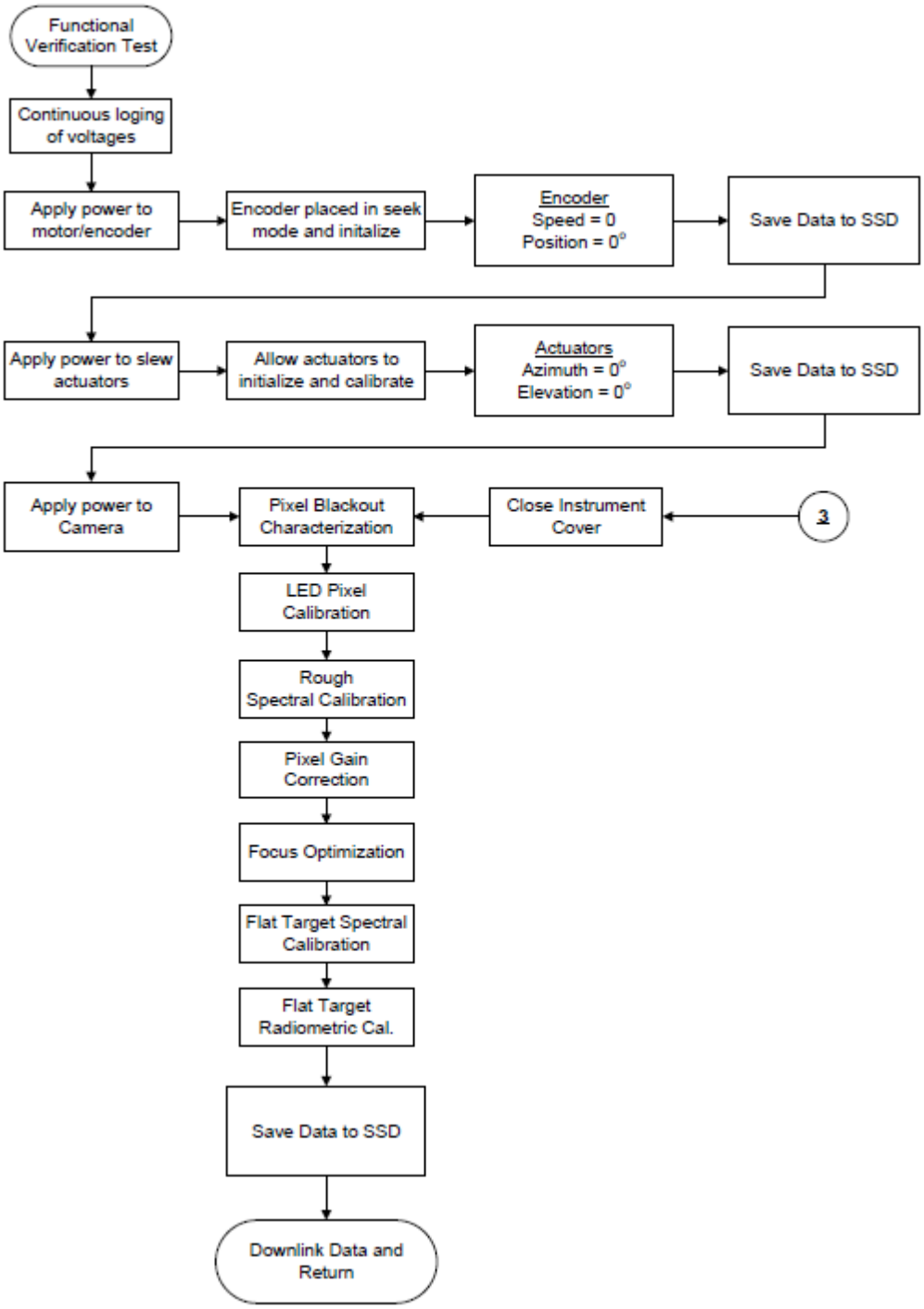

Figure 17: Space-Based CTEx Functional Verification Test Flow Diagram

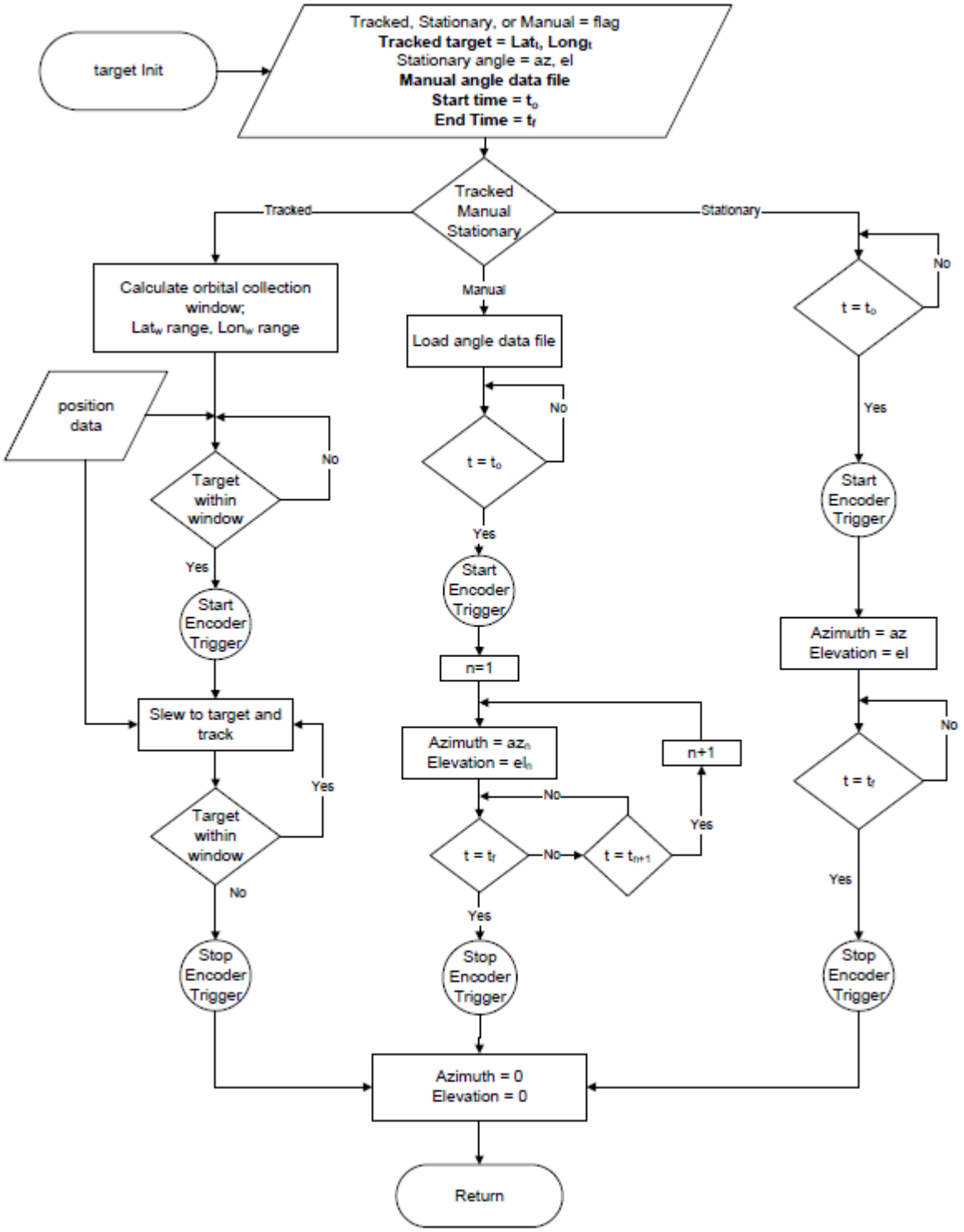

Figure 18: Space-Based CTEx Slewing Control Function Flow Diagram

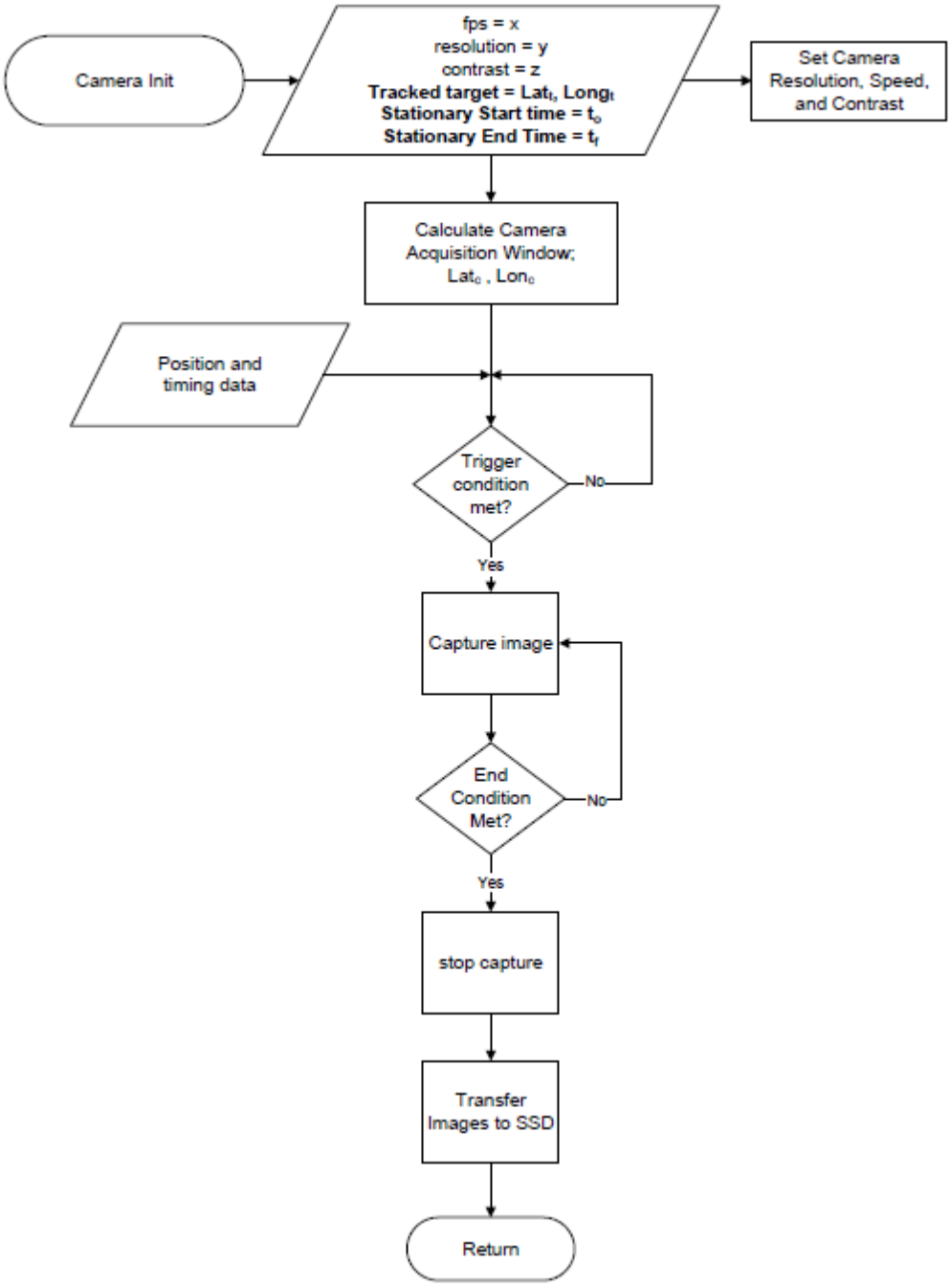

Figure 19: Space-Based CTEx Camera Control Function Flow Diagram

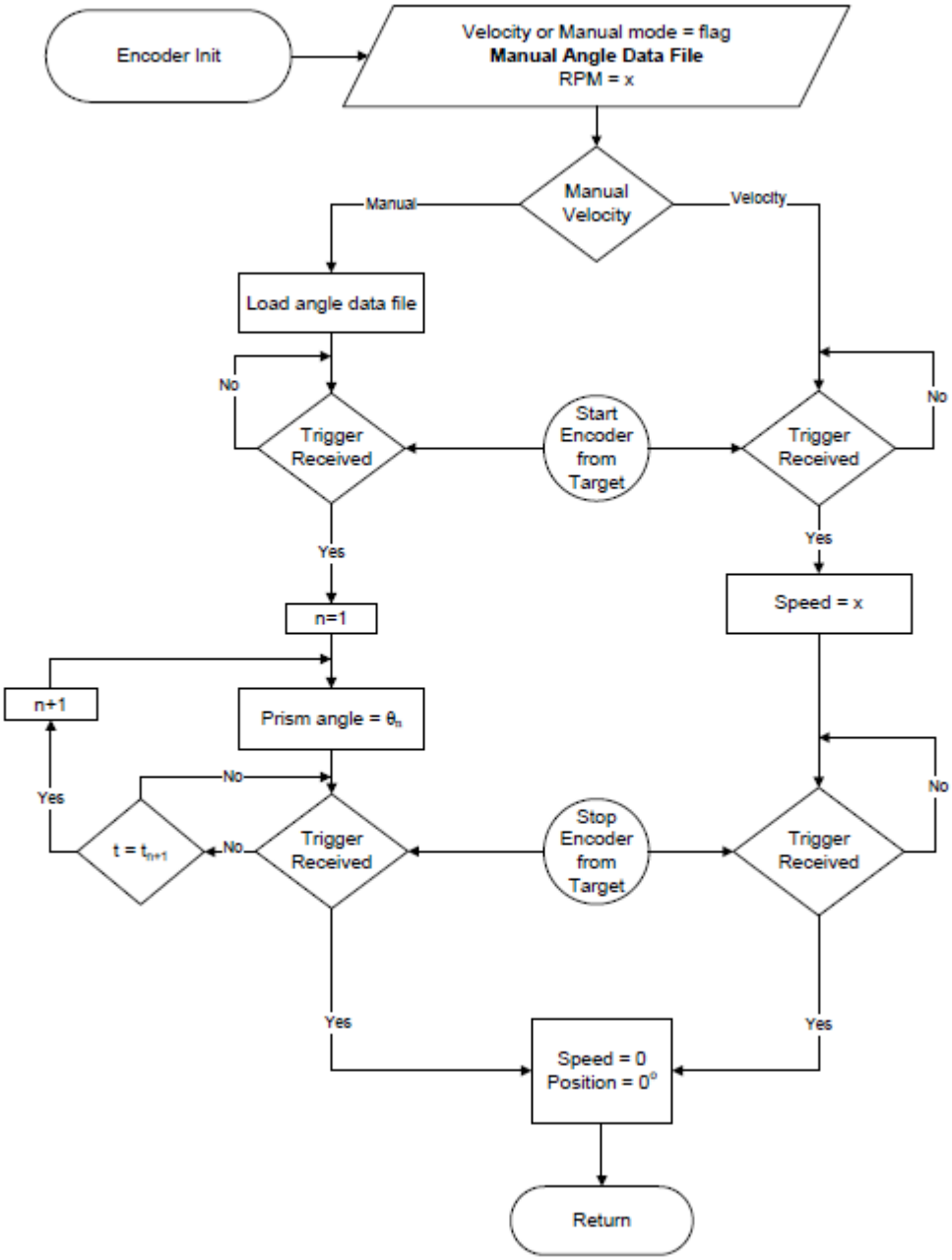

Figure 20: Space-Based CTEx Prism Control Function Flow Diagram